J. Fluid Mech. (1987), *vol.* 185, *pp.* 361–383
Printed in Great Britain

Influence of viscosity on the capillary instability of a stretching jet

By I. FRANKEL AND D. WEIHS
Dept. of Aeronautical Engineering, Technion, Haifa 32000, Israel

(Received 8 December 1986 and in revised form 12 May 1987)

The hydrodynamic stability of a rapidly elongating, viscous liquid jet such as obtained in shaped charges is presented. The flow field depends on three characteristic timescales associated with the growth of perturbations (due essentially to the effect of the surface tension), the elongation of the jet, and the inward diffusion of vorticity from the free surface, respectively. The latter process introduces a time lag resulting in the current values of the free-surface perturbation and its time derivative being a function of their past history. Solutions of the integro-differential equation for the evolution of disturbances exhibit a novel dual role played by the viscosity: besides the traditional damping effect it is associated with a destabilizing mechanism in the elongating jet. The wavelength of maximum instability is also a function of time elapsed since the jet formation, longer wavelengths becoming dominant at later stages. Understanding of these instability processes can help in both promoting and delaying instability as required by specific applications.

1. Introduction

In a recent study (Frankel & Weihs 1985, hereinafter referred to as FW), the stability of an inviscid jet with linearly increasing axial velocity was examined. Such jets appear in shaped charges, as well as for fibre spinning and emulsification processes. While the latter applications can conceivably be studied under creeping-flow assumptions (Tomotika 1936; Mikami, Cox & Mason 1975) the shaped-charge jet moves at velocities of the order of 10^3 m/s and internal axial velocity gradients of the order of 10^4 s^{-1}, so that the effects of inertia have to be included.

The superior penetration capabilities of hollow and shaped charges have been recognized for almost 200 years. The first quantitative analysis of the hydrodynamical principles involved and the first performance predictions were produced by Birkhoff *et al.* (1948) during World War II. One of the main conclusions of these studies was that penetration of solid targets would increase linearly with jet length at the point of impact – this being the motivation for forming elongating jets in the first place. Thus, for a given charge, increasing the distance from the target at jet formation should increase penetration. However, beyond a certain distance the penetration actually decreases. This has been shown to be a result of hydrodynamic instability of the jet (FW).

In the present paper the solution in FW is generalized to include the effect of liquid viscosity. We thus study the respective influence of surface tension, inertia and viscosity of the liquid, and the strain rate in the jet, on the temporal evolution of infinitesimal perturbations in the unsteady basic elongational flow.

In the applications mentioned previously the growth of perturbations is a key factor: non-uniformity and break-up of the jet constitutes one of the major

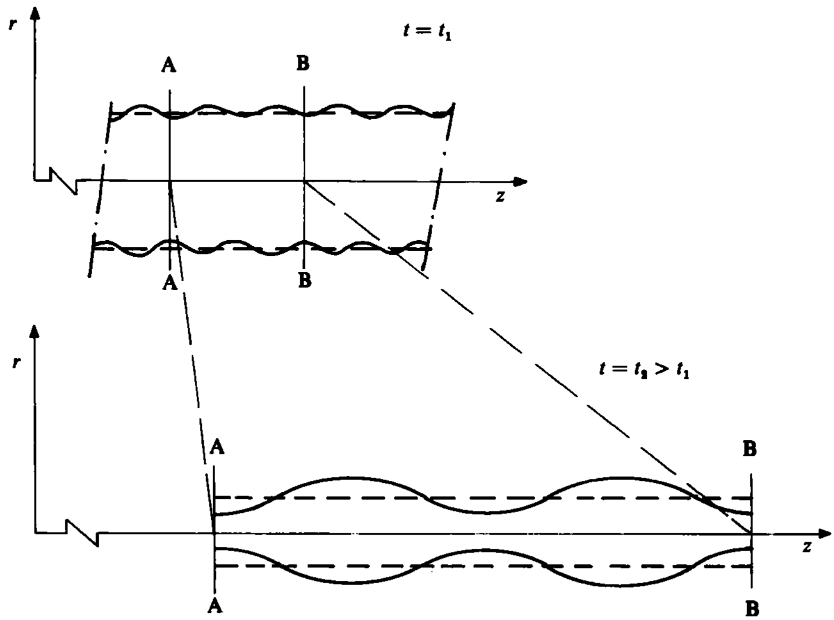

FIGURE 1. Schematic description of the stretching jet.

limitations on the penetration capability of shaped charges, and is to be avoided in polymer-fibre-spinning processes. In optical-fibre manufacturing, any deviations from a perfect circular cylindrical shape (due to growth of perturbations) tend to increase undesirable light scattering and are thus detrimental to the optical quality of the product.

In §2 we describe the flow field and the stability problem. In §3 we obtain the 'equation of motion' for the free surface of the perturbed jet. This equation contains integrals over the vorticity distribution in the jet. Having determined the relation between the vorticity distribution and the free-surface perturbations in §4, we find the evolution equation for the amplitude of perturbations in §5. The solutions of this equation are presented in §6. We describe the temporal evolution of the free-surface perturbations and the vorticity distribution within the jet, and the dependence of the amplification on the wavelength of perturbations. The general solution, which is valid for any combination of the parameters, enables establishing of the range of validity of the various approximations ('creeping flow', ideal jet, etc.).

2. Formulation of the problem

2.1. *The basic flow field*

The velocity field in the unperturbed stretching jet is one of an unsteady uniaxial extension (FW):

$$U_0 = -\frac{Kr}{2(Kt+1)}, \quad W_0 = \frac{Kz}{Kt+1}, \qquad (1a,b)$$

where r, z are cylindrical coordinates, U_0 and W_0 are, respectively, the radial and axial velocity components, and K is the axial velocity gradient at $t = 0$ (figure 1).

As a result of the stretching, the jet radius decreases with time as

$$a(t) = \frac{a_0}{(Kt+1)^{\frac{1}{2}}}, \tag{2}$$

where a_0 is the radius at $t = 0$. The pressure distribution within the unperturbed jet is

$$P_0 = \frac{3}{8}\frac{\rho K^2 a^2}{(Kt+1)^2}\left(1-\frac{r^2}{a^2}\right)+\frac{\sigma}{a}-\frac{\mu K}{Kt+1}, \tag{3}$$

where ρ, μ and σ are, respectively, the density, viscosity and coefficient of surface tension. The above expression is obtained via integration of the Navier–Stokes equation in conjunction with the free-surface dynamic boundary condition

$$P_0 = \frac{\sigma}{a}+2\mu\frac{\partial U_0}{\partial r}, \quad r = a. \tag{4}$$

2.2. *Perturbation equations*

It has been demonstrated in FW that only axisymmetric perturbations can be monotonically divergent for an ideal jet. We thus assume the perturbed flow field to be axisymmetric in the present case also. The velocity components are

$$U = U_0+u, \quad W = W_0+w, \tag{5a, b}$$

and the pressure distribution is

$$P = P_0+p. \tag{6}$$

u and w are, respectively, the radial and axial velocity perturbations, and p is the pressure perturbation. Substitution of the velocity and pressure fields into the continuity and Navier–Stokes equations, and subtraction of the terms which belong to the basic solution, lead to

$$\frac{1}{r}\frac{\partial}{\partial r}(ru)+\frac{\partial w}{\partial z} = 0, \tag{7}$$

$$\rho\left(\frac{\partial u}{\partial t}+U_0\frac{\partial u}{\partial r}+W_0\frac{\partial u}{\partial z}+u\frac{\partial U_0}{\partial r}\right) = -\frac{\partial P}{\partial r}+\mu\left\{\frac{\partial}{\partial r}\left[\frac{1}{r}\frac{\partial}{\partial r}(ru)\right]+\frac{\partial^2 u}{\partial z^2}\right\}, \tag{8}$$

$$\rho\left(\frac{\partial w}{\partial t}+U_0\frac{\partial w}{\partial r}+W_0\frac{\partial w}{\partial z}+w\frac{\partial W_0}{\partial z}\right) = -\frac{\partial p}{\partial z}+\mu\left[\frac{1}{r}\frac{\partial}{\partial r}\left(r\frac{\partial w}{\partial r}\right)+\frac{\partial^2 w}{\partial z^2}\right], \tag{9}$$

neglecting second-order terms in the velocity perturbations. Cross-differentiating (8) and (9) and subtracting, we eliminate p and obtain

$$\frac{\partial \zeta'}{\partial t}+U_0\frac{\partial \zeta'}{\partial r}+W_0\frac{\partial \zeta'}{\partial z}+\frac{K}{Kt+1}\zeta' = \nu\left(\frac{\partial^2\zeta'}{\partial r^2}-\frac{1}{r}\frac{\partial \zeta'}{\partial r}+\frac{\partial^2\zeta'}{\partial z^2}\right), \tag{10}$$

where

$$\zeta' = \hat{\zeta}r. \tag{11}$$

$\hat{\zeta} = (\partial u/\partial z) - (\partial w/\partial r)$ is the vorticity and $\nu = \mu/\rho$ is the kinematic viscosity. In terms of the Stokes stream function, (7)–(9) can be written as (10) and

$$\frac{\partial^2\psi}{\partial r^2} - \frac{1}{r}\frac{\partial\psi}{\partial r} + \frac{\partial^2\psi}{\partial z^2} = \zeta'. \tag{12}$$

Some further simplification is achieved through a transformation to an approximate Lagrangian description where (FW)

$$r = r_0(Kt+1)^{-\frac{1}{2}}, \quad z = z_0(Kt+1) \tag{13a,b}$$

The coefficients in the equations which result from changing the independent variables in (9) and (12) by the transformation (13) are functions of r_0 and t only. We can thus assume standing-wave solutions of the form

$$\zeta = \bar{\zeta}(r_0, t) \sin k_0 z_0 \tag{14}$$

and
$$\psi = \bar{\psi}(r_0, t) \sin k_0 z_0, \tag{15}$$

where $\zeta = (Kt+1)\zeta'$. k_0 is the wavenumber at $t = 0$ of an axial perturbation which stretches with the jet (and its current wavenumber at time t is $k_0(Kt+1)^{-1}$). One obtains for $\bar{\zeta}$ and $\bar{\psi}$

$$\frac{1}{Kt+1}\frac{\partial\bar{\zeta}}{\partial t} = \nu\left[\frac{\partial^2\bar{\zeta}}{\partial r_0^2} - \frac{1}{r_0}\frac{\partial\bar{\zeta}}{\partial r_0} - \frac{k_0^2}{(Kt+1)^3}\bar{\zeta}\right] \tag{16}$$

and
$$\frac{\partial^2\bar{\psi}}{\partial r_0^2} - \frac{1}{r}\frac{\partial\bar{\psi}}{\partial r_0} - \frac{k_0^2}{(Kt+1)^3}\bar{\psi} = \frac{\bar{\zeta}}{(Kt+1)^2}. \tag{17}$$

Equations (16) and (17) can be written in non-dimensional form as

$$\frac{1}{\tau}\frac{\partial\bar{\zeta}^*}{\partial\tau} = \frac{1}{R}\left(\frac{\partial^2\bar{\zeta}^*}{\partial r_0^2} - \frac{1}{r_0}\frac{\partial\bar{\zeta}^*}{\partial r_0} - \chi^2\bar{\zeta}^*\right) \tag{18a}$$

and
$$\frac{\partial^2\bar{\psi}^*}{\partial r_0^2} - \frac{1}{r_0^*}\frac{\partial\bar{\psi}^*}{\partial r_0^*} - \chi^2\bar{\psi}^* = \frac{\bar{\zeta}^*}{\tau^2}, \tag{18b}$$

where
$$r_0 = a_0 r_0^*, \quad z_0 = a_0 z_0^*, \quad \tau = Kt+1, \quad \bar{\zeta} = Ka_0\bar{\zeta}^*,$$
$$\bar{\psi} = Ka_0^3\bar{\psi}^*, \quad u = Ka_0 u^*, \quad w = Ka_0 w^*, \quad p = \rho K^2 a_0^2 p^*,$$

and $R = Ka_0^2/\nu$ is the ratio between inertial and viscous effects or, equivalently, between the respective timescales for vorticity diffusion (a_0^2/ν) and the jet elongation $(1/K)$, and

$$\chi = \frac{k_0 a_0}{(Kt+1)^{\frac{3}{2}}} \tag{19}$$

is the non-dimensional instantaneous wavenumber.

For simplicity, the asterisks are omitted in the following. Unless otherwise stated the various quantities are non-dimensional.

The kinematic boundary condition on the jet surface is

$$U = \frac{\mathrm{D}b}{\mathrm{D}t} = \frac{\partial b}{\partial t} + \boldsymbol{u}\cdot\nabla b \quad \text{at } r = b, \tag{20}$$

where $r = b(z,t)$ is the free surface of the perturbed jet.

The dynamic boundary conditions are

zero tangential stress: $$\tau_t = 0 \quad \text{at } r = b, \tag{21}$$

and $$\tau_n = -\sigma\left(\frac{1}{R_1}+\frac{1}{R_2}\right) \quad \text{at } r = b, \tag{22}$$

i.e. the normal stress is balanced by the effect of surface tension. R_1 and R_2 are the (dimensional) principal radii of curvature.

Assuming axisymmetric standing-wave perturbations of the free surface (as in (14) and (15))

$$b(z_0, t) = a(t)[1+\eta(t)\cos k_0 z_0 a_0]. \tag{23}$$

Substituting (5) and (6) in conjunction with (23) and linearizing we obtain, for $r_0 = 1$,

$$u \approx \frac{a(t)}{a_0}\eta'(\tau)\cos k_0 z_0 a_0 \tag{24}$$

and writing τ_n and τ_t in terms of the stress tensor in cylindrical coordinates,

$$\frac{1}{\tau}\frac{\partial u}{\partial z_0}+\tau^{\frac{1}{2}}\frac{\partial w}{\partial r_0} = -3\frac{\chi}{\tau}\eta(\tau)\sin k_0 z_0 a_0, \tag{25}$$

$$p-2\frac{\tau^{\frac{1}{2}}}{R}\frac{\partial u}{\partial r_0} \approx -\frac{3}{4}\left[T\tau^{\frac{1}{2}}(1-\chi^2)-\frac{1}{\tau^3}\right]\eta(\tau)\cos k_0 z_0 a_0, \tag{26}$$

where $$T = \frac{4}{3}\frac{\sigma}{\rho K^2 a_0^3}$$

expresses the relative effects of the surface tension and the inertia of the jet. T is also the ratio between the squares of the capillary and elongational timescales ($(\sigma/\rho a_0^3)^{\frac{1}{2}}$ and K^{-1} respectively).

In addition to the free surface-conditions (24)–(26), axial symmetry and the requirement of a non-singular solution at $r = 0$ result in

$$r_0 = 0: \quad u = 0, \tag{27a}$$

$$r_0 = 0: \quad \frac{\partial w}{\partial r_0} = 0. \tag{27b}$$

3. Evolution of perturbations of the jet surface

The general solution of (17) is

$$\bar{\psi} = r_0 I_1(\chi r_0)\left[A(\tau)+\frac{1}{\tau^2}\int_0^{r_0} K_1(\chi r_0')\,\bar{\zeta}(r_0',\tau)\,\mathrm{d}r_0'\right] + r_0 K_1(\chi r_0)\left[B(\tau)-\frac{1}{\tau^2}\int_0^{r_0} I_1(\chi r_0')\,\bar{\zeta}(r_0',\tau)\,\mathrm{d}r_0'\right], \tag{28}$$

where I_1 and K_1 are the first-order modified Bessel functions of the first and second kind respectively.

The velocity components in non-dimensional Lagrangian form are

$$u = \frac{1}{\tau^{\frac{1}{2}} r_0} \frac{\partial \bar{\psi}}{\partial z_0}, \quad w = -\frac{\tau}{r_0} \frac{\partial \bar{\psi}}{\partial r_0}.$$

The pressure perturbation is obtained by integration of (8) and (9). In the Lagrangian non-dimensional variables it is

$$p = \frac{1}{k_0 a_0 r_0} \frac{\partial}{\partial r_0} \left[\frac{\partial}{\partial \tau} (\tau^2 \bar{\psi}) - \frac{\tau}{R} \bar{\zeta} \right] \cos(k_0 a_0 z_0). \tag{29}$$

Substitution of the expressions (28) and (29) into the boundary conditions (24)–(26) leads to a linear system of three equations for the three unknown functions: $\bar{\zeta}(r_0, \tau)$, $\eta(\tau)$ and $A(\tau)$. The latter can be eliminated between the equations that correspond to the kinematic boundary condition and the condition for the tangential stress on the free surface. In addition we obtain the relation

$$\bar{\zeta}(1, \tau) = \frac{k_0 a_0}{\tau^2} [3\eta(\tau) - 2\tau\eta'(\tau)] = f(\tau) \tag{30}$$

between the intensity of the 'vorticity source' on the free surface and the perturbation amplitude.

A free surface of a viscous fluid is a vorticity source since an irrotational flow cannot in general satisfy the requirement that the tangential stress vanishes there. (The basic flow is an exception which is due to the circular cylindrical shape of the unperturbed jet.) It is a weaker source than a solid body where the failure to satisfy the 'no slip' condition results in a finite discontinuity in the velocity, which corresponds to a vortex sheet of infinite intensity. In the case of a free surface the irrotational flow involves only a finite discontinuity in the tangential stress, which forms a vortex sheet of finite intensity (Batchelor 1967, p. 364).

Substitution of the expression for $A(\tau)$ in the equation that corresponds to the dynamic boundary condition for the normal stress on the free surface, making use of the relation $K_0(\chi) I_1(\chi) + I_0(\chi) K_1(\chi) = 1/\chi$ (Abramowitz & Stegun 1965, p. 375), we obtain an equation for $\eta(\tau)$ which includes the term

$$\int_0^1 I_1(\chi r_0') \frac{\partial \bar{\zeta}}{\partial \tau}(r_0', \tau) \, dr_0'.$$

The equation thus obtained can be simplified considerably by replacing the time derivative $\partial\bar{\zeta}/\partial\tau$ in the above term. To this end we express $\partial\bar{\zeta}/\partial\tau$ employing (18*a*) and integrate by parts twice in conjunction with the conditions

$$\lim_{r_0 \to 0} \bar{\zeta} = 0, \quad \lim_{r_0 \to 0} \frac{\partial \bar{\zeta}}{\partial r_0} = 0$$

which result from (27). Eventually we find that

$$\int_0^1 I_1(\chi r_0') \frac{\partial}{\partial \tau} \bar{\zeta}(r_0', \tau) \, dr_0' = \frac{\tau}{R} I_1(\chi) \left(\frac{\partial \bar{\zeta}}{\partial r_0} \right)_{r_0 = 1} - \frac{\tau \chi}{R} \bar{\zeta}(1, \tau).$$

Substitution along with (30) for $\bar{\zeta}(1,\tau)$ leads to the equation of motion for the free surface of the perturbed jet:

$$\frac{I_0}{\tau\chi I_1}\eta''(\tau)+\left[-\frac{3}{2\tau^2}-\frac{2}{R}+\left(\frac{4\chi}{R}-\frac{1}{\tau^2\chi}\right)\frac{I_0}{I_1}+\frac{3}{2\tau^2}\frac{I_0^2}{I_1^2}\right]\eta'(\tau)-\frac{3}{4}\left[T\tau^{\frac{1}{2}}(1-\chi^2)-\frac{1}{\tau^3}+\frac{4\chi}{R\tau}\frac{I_0}{I_1}\right]\eta(\tau)$$

$$+\left[\frac{3}{2}\frac{1}{\tau^{\frac{5}{2}}}\frac{I_0}{I_1^2}+2\frac{\chi}{R\tau^{\frac{1}{2}}}\frac{1}{I_1}\right]\int_0^1 I_1(\chi r_0')\,\bar{\zeta}(r_0',\tau)\,\mathrm{d}r_0'-\frac{3}{2}\frac{1}{\tau^{\frac{5}{2}}I_1}\int_0^1 r_0' I_1(\chi r_0')\,\bar{\zeta}(r_0',\tau)\,\mathrm{d}r_0'=0, \quad (31)$$

where $I_0=I_0(\chi)$, $I_1=I_1(\chi)$.

The last two terms on the left-hand side of (31) include the contribution of vorticity distribution to the rate of energy dissipation in the jet (cf. Lamb 1932, p. 581).

For an inviscid jet $\nu=0$ and $R\to\infty$ and the equation for the vorticity (18*a*) assumes the form $\partial\bar{\zeta}/\partial\tau=0$. Also, in this case, the dynamic boundary condition (21) is satisfied identically and the velocity field no longer needs to satisfy (25).

The flow field can thus be assumed irrotational $\bar{\zeta}=0$ (cf. the discussion of the dependence of $\bar{\zeta}$ on R in the next section). We thus obtain in this limit

$$\eta''(\tau)+\left[\frac{3}{2}\frac{\chi I_0}{I_1}-1-\frac{3}{2}\frac{\chi I_1}{I_0}\right]\frac{\eta'(\tau)}{\tau}+\frac{3}{4}\frac{1}{\tau^2}\frac{\chi I_1}{I_0}[T\tau^{\frac{7}{2}}(1-\chi^2)-1)]\,\eta(\tau)=0, \quad (32)$$

as obtained in FW for the perturbations of an inviscid jet.

4. The vorticity in the perturbed jet

$\bar{\zeta}(r_0,t)$ is described by (18*a*):

$$\frac{\partial\bar{\zeta}}{\partial\tau}=\frac{\tau}{R}\left(\frac{\partial^2\bar{\zeta}}{\partial r_0^2}-\frac{1}{r_0}\frac{\partial\bar{\zeta}}{\partial r_0}-\chi^2\bar{\zeta}\right),$$

with boundary conditions (30),

$$r_0=1:\quad \bar{\zeta}(1,\tau)=\frac{k_0a_0}{\tau^2}[3\eta(\tau)-2\tau\eta'(\tau)]=f(\tau),$$

and
$$r_0=0:\quad \lim_{r_0\to 0}\frac{\bar{\zeta}}{r_0}=0, \quad (33)$$

which assures the regularity of the solution on the jet axis. The equation for $\bar{\zeta}$ is parabolic with initial condition

$$\tau=\tau_0:\quad \bar{\zeta}(r_0,\tau)=g(r_0). \quad (34)$$

The main difficulty in solving the above problem arises from the fact that the coefficients in (18*a*) are functions of both r_0 and τ. We therefore define the new variables τ_1 and $\bar{\zeta}_1(r_0,\tau_1)$:

$$\tau_1=\frac{1}{2}\frac{\tau^2-\tau_0^2}{R},\quad \bar{\zeta}(r_0,\tau)=r_0\exp\left(\frac{k_0^2a_0^2}{R\tau}\right)\bar{\zeta}_1(r_0,\tau_1). \quad (35a,b)$$

In these new variables one obtains

$$\frac{\partial \bar{\zeta}_1}{\partial \tau_1} = \frac{\partial^2 \bar{\zeta}_1}{\partial r_0^2} + \frac{1}{r_0}\frac{\partial \bar{\zeta}_1}{\partial r_0} - \frac{\bar{\zeta}_1}{r_0^2}, \tag{36}$$

which is to be solved in the domain $0 \leqslant r_0 \leqslant 1$, $0 < \tau_1 < \infty$ in conjunction with the boundary conditions

$$r_0 = 0: \quad \bar{\zeta}_1(r_0, \tau_1) = 0, \tag{37a}$$

$$r_0 = 1: \quad \bar{\zeta}_1(r_0, \tau_1) = \bar{f}_1(\tau_1), \tag{37b}$$

and the initial condition

$$\tau_1 = 0: \quad \bar{\zeta}_1(r_0, 0) = \bar{g}_1(r_0). \tag{37c}$$

(The relations between $\bar{f}_1(\tau_1)$ and $f(\tau)$, and between $\bar{g}_1(r_0)$ and $g(r_0)$ are readily obtained from the transformation (35).)

The linearity allows for a decomposition

$$\bar{\zeta}_1 = \bar{\zeta}_{11} + \bar{\zeta}_{12}, \tag{38}$$

where both $\bar{\zeta}_{11}$ and $\bar{\zeta}_{12}$ satisfy (36). $\bar{\zeta}_{11}$ is the solution for the problem with a homogeneous initial condition

$$\bar{\zeta}_{11}(0, \tau_1) = 0, \quad \bar{\zeta}_{11}(1, \tau_1) = \bar{f}_1(\tau_1), \quad \bar{\zeta}_{11}(r_0, 0) = 0, \tag{39a, b, c}$$

while $\bar{\zeta}_{12}$ is the solution for the problem with a homogeneous boundary condition

$$\bar{\zeta}_{12}(0, \tau_1) = 0, \quad \bar{\zeta}_{12}(1, \tau_1) = 0, \quad \bar{\zeta}_{12}(r_0, 0) = \bar{g}_1(r_0) \tag{40a, b, c}$$

4.1. *The homogeneous initial condition*

Defining $z_{11}(r_0, S) = L[\bar{\zeta}_{11}(r_0, \tau_1)]$ as the Laplace transform of $\bar{\zeta}_{11}(r_0, \tau_1)$, we obtain

$$z_{11}(r_0, S) = \frac{I_1(r_0 S^{\frac{1}{2}})}{S I_1(S^{\frac{1}{2}})} S F(S), \tag{41}$$

where $F(S) = L[\bar{f}_1(\tau_1)]$.

The inverse transforms are

$$L^{-1}[SF(S)] = \bar{f}_1(\tau_1) + \bar{f}_1(0)\,\delta(\tau_1), \tag{42a}$$

with $\delta(\tau_1)$ the Dirac delta function, and

$$L^{-1}\left[\frac{I_1(r_0 S^{\frac{1}{2}})}{S I_1(S^{\frac{1}{2}})}\right] = r_0 + 2\sum_{k=1}^{\infty} \frac{J_1(d_k r_0)}{d_k J_0(d_k)} \exp(-d_k^2 \tau_1), \tag{42b}$$

where J_0 and J_1 are the Bessel functions of the first kind and of the zeroth and first order respectively, and $d_k, k = 1, 2, \ldots$, are the positive zeros of J_1 (Frankel 1984). Equation (42*b*) is identical with the expression for the velocity field in a viscous liquid that is initially at rest in a circular cylinder of unit radius. At $\tau_1 = 0^+$ the cylinder starts rotating with unit velocity (cf. Gray, Mathews & MacRobert 1922, p. 249; Goldstein 1932). $\bar{\zeta}_{11}$ is thus analogous to the velocity field obtained when the cylinder rotates with the velocity $\bar{f}_1(\tau_1)$ starting from rest at $\tau_1 = 0^+$.

$\bar{\zeta}_{11}$ is found by substitution of (42a, b) in the convolution theorem for Laplace transform:

$$\bar{\zeta}_{11}(r_0, \tau_1) = L^{-1}[SF(S)] * L^{-1}\left[\frac{I_1(r_0 S^{\frac{1}{2}})}{SI_1(S^{\frac{1}{2}})}\right]$$

$$= r_0 \bar{f}_1(\tau_1) + 2\int_0^{\tau_1} [f_1'(\tau_1') + \delta(\tau_1') f_1(0)] \left[\sum_{k=1}^{\infty} \frac{J_1(d_k r_0)}{d_k J_0(d_k)} \exp(-d_k^2(\tau_1 - \tau_1'))\right] d\tau_1'.$$

Changing the order of integration and summation and integrating by parts, the expression is recast in the form

$$\bar{\zeta}_{11} = \left[r_0 + 2\sum_{k=1}^{\infty} \frac{J_1(d_k r_0)}{d_k J_0(d_k)}\right] \bar{f}_1(\tau_1) - 2\sum_{k=1}^{\infty} \frac{d_k J_1(d_k r_0)}{J_0(d_k)} \int_0^{\tau_1} \bar{f}_1(\tau_1') \exp(-d_k^2(\tau_1 - \tau_1'))\, d\tau_1'. \tag{43}$$

4.2. *The homogeneous boundary condition*

We consider the evolution of the vorticity field from some initial distribution $\bar{g}_1(r_0)$. The following solution assumes that $g_1(r_0)$ satisfies Dirichlet conditions (which from a physical point of view does not constitute a severe restriction on the applicability of the resulting solution).

An interesting case where this assumption is not satisfied is the 'instantaneous vorticity source' – i.e. the vorticity distribution that develops from a cylindrical vortex sheet. This case was shown to correspond to the Green-function approach, leading to results equivalent to the following. Assuming $\bar{\zeta}_{12}$ to be representable by an eigenfunction series expansion we obtain

$$\bar{\zeta}_{12} = \sum_{k=1}^{\infty} \bar{A}_k \exp(-d_k^2 \tau_1) J_1(d_k r_0),$$

which satisfies (36) and (40a, b). (In order to satisfy the initial condition (40c) $\bar{A}_k$ are chosen as the coefficients in the Bessel–Fourier expansion of $\bar{g}_1(r_0)$, hence

$$\bar{\zeta}_{12} = 2\sum_{k=1}^{\infty} \frac{J_1(d_k r_0)}{J_0^2(d_k)} \exp(-d_k^2 \tau_1) \int_0^1 r_0' J_1(d_k r_0') \bar{g}_1(r_0')\, dr_0'. \tag{44}$$

The homogeneous-boundary-condition case is analogous to the following problem: A viscous liquid is placed in a stationary circular cylinder. By a suitable stirring action, a stress distribution $\tau_{r\theta}$ is formed, which maintains a circular flow with the velocity $v = \bar{g}_1(r_0)$. Thus $\bar{\zeta}_{12}$ describes the damping of the velocity field $v(r_0, \tau_1)$ after cessation of the stirring action.

The contribution to the vorticity distribution which results from the initial distribution is independent of the evolution of the free-surface perturbations. This is to be anticipated since the formulation of the problem for $\bar{\zeta}_{12}$ ((36) and (40a–c)) does not include any dependence on η. Similar phenomena have been pointed out by Prosperetti in the context of surface waves on viscous liquids (1976) and the vibrations of drops and bubbles (1980).

4.3. *Dependence of the vorticity distribution on R*

Substituting $\bar{\zeta}_{11}$, (43), and $\bar{\zeta}_{12}$, (44), in (38), and making use of the transformation (35), we recover

$$\bar{\zeta}(r_0,\tau) = r_0\left[r_0 + 2\sum_{k=1}^{\infty}\frac{J_1(d_k r_0)}{d_k J_0(d_k)}\right]f(\tau)$$

$$-\frac{2}{R}r_0\exp\left(\frac{k_0^2 a_0^2}{R\tau}\right)\sum_{k=1}^{\infty}\frac{d_k J_1(d_k r_0)}{J_0(d_k)}\exp\left(-\frac{d_k^2\tau^2}{2R}\right)\int_{\tau_0}^{\tau}\exp\left(\frac{d_k^2\tau'^2}{2R}-\frac{k_0^2 a_0^2}{R\tau'}\right)f(\tau')\,d\tau'$$

$$+r_0\exp\left[-\frac{k_0^2 a_0^2}{R}\left(\frac{1}{\tau_0}-\frac{1}{\tau}\right)\right]\sum_{k=1}^{\infty}A_k J_1(d_k r_0)\exp\left[-\frac{d_k^2}{2R}(\tau^2-\tau_0^2)\right], \tag{45}$$

where
$$A_k = \frac{2}{J_0^2(d_k)}\int_0^1 g(r_0')J_1(d_k r_0')\,dr_0'.$$

Insight into the physical phenomena involved in the evolution of the jet perturbations can be gained by studying the above vorticity field.

The first term on the right-hand side of (45) is independent of R. The series that appears in this term is the Bessel–Fourier expansion of

$$h(r_0) = \begin{cases}-r_0, & 0 \leqslant r_0 < 1,\\ 0, & r_0 = 1,\end{cases}$$

and hence

$$r_0\left[r_0 + 2\sum_{k=1}^{\infty}\frac{J_1(d_k r_0)}{d_k J_0(d_k)}\right]f(\tau) = \begin{cases}0, & 0 \leqslant r_0 < 1,\\ f(\tau), & r_0 = 1,\end{cases} \tag{46}$$

which assures that the boundary condition (30) is satisfied.

The second term in (45) represents the distribution due to the inward diffusion of vorticity from the free surface. Since this diffusion process takes a finite time (for finite R), this term contains contributions of the 'source intensity' $f(\tau)$ at times $\tau' < \tau$.

The last term represents the effect of the initial distribution. As mentioned above, this contribution is not affected by the evolution of the surface perturbations, and it hence is independent of $f(\tau)$.

We now examine the limiting cases: $R \to 0, \infty$:

(i) $R \to \infty$

In this case the second term on the right-hand side of (45) vanishes and the third assumes the form

$$2r_0\sum_{k=1}^{\infty}\frac{J_1(d_k r_0)}{J_0^2(d_k)}\int_0^1 g(r_0')J_1(d_k r_0')\,dr_0' = \begin{cases}g(r_0), & 0 \leqslant r_0 < 1,\\ 0, & r_0 = 1.\end{cases}$$

In accordance with (46) we have

$$\bar{\zeta}(r_0,\tau) = \begin{cases}g(r_0), & 0 \leqslant r_0 < 1,\\ f(\tau), & r_0 = 1,\end{cases} \tag{47}$$

i.e. in the absence of diffusion the vorticity distribution in the interior of the jet remains unchanged with time, in accordance with Kelvin's theorem.

(ii) $R \to 0 (K \neq 0)$

In this case, the last term on the right-hand side of (45) vanishes for all $\tau > \tau_0$, i.e. any initial vorticity distribution disappears instantaneously.

The limiting form for $R \to 0$ of the second term is obtained by integrating it by parts twice. We thus obtain

$$\bar{\zeta}(r_0, \tau) = r_0 \left[r_0 + 2 \sum_{k=1}^{\infty} \frac{J_1(d_k r_0)}{d_k J_0(d_k)} \right] f(\tau) - 2r_0 f(\tau) \sum_{k=1}^{\infty} \frac{d_k J_1(d_k r_0)}{(\chi^2 + d_k^2) J_0(d_k)}.$$

The sum of the second series on the right-hand side is

$$-2 \sum_{k=1}^{\infty} \frac{d_k J_1(d_k r_0)}{(\chi^2 + d_k^2) J_0(d_k)} = \begin{cases} \dfrac{I_1(\chi r_0)}{I_1(\chi)}, & 0 \leqslant r_0 < 1, \\ 0, & r_0 = 1. \end{cases}$$

Consequently
$$\bar{\zeta}(r_0, \tau) = \frac{f(\tau)}{I_1(\xi)} r_0 I_1(\chi r_0). \tag{48}$$

The result is identical with the one which is obtained for an elongating viscous jet in the 'creeping flow' approximation (Frankel 1984).

Thus the vorticity distribution depends only on the instantaneous 'source intensity' $f(\tau)$ on the free surface for all $\tau > \tau_0$. This is because for $R = 0$, the vorticity diffuses infinitely fast and therefore the vorticity distribution at any $\tau > \tau_0$ is independent of its distribution at any earlier instant $\tau' < \tau$.

The result can be anticipated from (18*a*). For any finite R this is a parabolic equation and hence the dependence of the current distribution on the 'history'. As $R \to 0$ (18*a*) becomes an ordinary one and the boundary conditions (30) and (33) suffice to determine a unique solution. This solution cannot satisfy any additional (initial) conditions.

5. Evolution of perturbations

Substituting the expressions for $\bar{\zeta}(r_0, \tau)$, (45), and for $f(\tau)$, (30), performing the integrations over the vorticity distribution in the equation of motion (31), and applying various relations for Bessel functions we obtain the evolution equation for $\eta(\tau)$, the perturbation amplitude:

$$\begin{aligned} &\frac{\tau^{\frac{1}{2}} I_0}{k_0 a_0 I_1} \eta''(\tau) + \left[-\frac{3}{2}\frac{1}{\tau^2} - \frac{2}{R} + \left(4\frac{\chi}{R} - \frac{1}{k_0 a_0 \tau^{\frac{1}{2}}} \right) \frac{I_0}{I_1} + \frac{3}{2} \frac{I_0^2}{\tau^2 I_1^2} \right] \eta'(\tau) \\ &\quad - \frac{3}{4} \left[T\tau^{\frac{1}{2}}(1-\chi^2) - \frac{1}{\tau^3} + 4\frac{\chi}{R\tau}\frac{I_0}{I_1} \right] \eta(\tau) + 2\frac{k_0^2 a_0^2}{R\tau^2} \exp\left(\frac{k_0^2 a_0^2}{R\tau} \right) \sum_{k=1}^{\infty} \left[\frac{2}{R} + \frac{3}{(\chi^2 + d_k^2)\tau^2} \right] \\ &\quad \times \frac{d_k^2}{\chi^2 + d_k^2} \exp\left(-\frac{d_k^2 \tau^2}{2R} \right) \int_{\tau_0}^{\tau} \exp\left(\frac{d_k^2 \tau'^2}{2R} - \frac{k_0^2 a_0^2}{R\tau'} \right) [3\eta(\tau') - 2\tau'\eta'(\tau')] \frac{d\tau'}{\tau'} \\ &= \frac{k_0^2 a_0^2}{\tau^2} \exp\left[-\frac{k_0^2 a_0^2}{R} \left(\frac{1}{\tau_0} - \frac{1}{\tau} \right) \right] \sum_{k=1}^{\infty} \frac{d_k J_0(d_k)}{\chi^2 + d_k^2} A_k \exp\left[-\frac{d_k^2}{2R}(\tau^2 - \tau_0^2) \right] \\ &\quad \times \left[\frac{2}{R} + \frac{3}{(\chi^2 + d_k^2)\tau^2} \right], \end{aligned} \tag{49}$$

with the coefficients A_k given by (45).

The series term on the left-hand side of (49) stems from the diffusion of vorticity inwards from the free surface. As this process requires finite time (at $R \neq 0$), we obtain an integro-differential evolution equation.

The vorticity distribution associated with the initial vorticity distribution is represented by the forcing term on the right-hand side of (49).

Previously we showed that the evolution equation for the case of an ideal jet (FW) can be obtained as a limiting case of (31) for $R \rightarrow \infty$. We now consider the other limit, namely, $R \rightarrow 0$.

Multiplying (49) by R, we obtain, when $R \rightarrow 0$, and $\tau > \tau_0$,

$$\left(4\chi\frac{I_0}{I_1}-2\right)\eta'(\tau)-3\left[S\tau^{\frac{1}{2}}(1-\chi^2)+4\frac{\chi}{\tau}\frac{I_0}{I_1}\right]\eta(\tau)+\lim_{R\rightarrow 0}\frac{2k_0^2a_0^2}{R\tau^2}\sum_{k=1}^{\infty}\left[\frac{2}{R}+\frac{3}{(\chi^2+d_k^2)\tau^2}\right]$$

$$\times\frac{d_k^2}{\chi^2+d_k^2}\exp\left(\frac{k_0^2a_0^2}{R\tau}-\frac{d_k^2\tau^2}{2R}\right)\int_{\tau_0}^{\tau}\exp\left(\frac{d_k^2\tau'^2}{2R}-\frac{k_0^2a_0^2}{R\tau'}\right)(3\eta-2\tau'\eta')\frac{d\tau'}{\tau'}=0, \quad (50)$$

where we define
$$S=\tfrac{1}{4}RT=\frac{1}{3}\frac{\sigma}{\mu K a_0}, \quad (51)$$

which represents the relative effects of surface tension and viscosity. The last term in (50) is treated like the term in (45) that led to (48). Integrating by parts twice and making use of various identities for Bessel functions we obtain

$$2\left[\chi^2\frac{I_0^2}{I_1^2}-(1-\chi^2)\right]\eta'(\tau)-3\left[S\tau^{\frac{1}{2}}(1-\chi^2)+\frac{\chi^2}{\tau}\left(\frac{I_0^2}{I_1^2}-\frac{I_0}{\chi I_1}-1\right)\right]\eta(\tau)=0, \quad (52)$$

which is identical with the 'creeping flow' solution (Frankel 1984).

In passing from (49) to (50) the 'acceleration' term which includes $\eta''(\tau)$ has been dropped. This is valid provided that

$$R\eta'' \ll \eta, S\eta, \eta'.$$

Returning to dimensional notation the first requirement is written

$$\frac{R}{(Kt_g)^2}=\frac{a_0^2}{\nu(Kt_g)\,t_g} \ll 1, \quad (53)$$

where t_g is a characteristic time for the growth of perturbations. Hence it is required that this timescale (t_g) be much larger than the timescale for the diffusion of vorticity (a_0^2/ν). This condition guarantees that the variations in the intensity of the free-surface vorticity source, which are induced by the growth of perturbations, will be much slower than the inward diffusion process. It is thus equivalent to the conditions for steady Stokes equations to be valid in an unsteady flow (Rosenhead 1963, p. 168).

Substituting $t_g \sim \mu a_0/\sigma$ which is the characteristic time for the growth of perturbations in a viscous capillary jet when the inertia effect is negligible, we see that the above condition is equivalent to:

$$S \ll \frac{1}{R^{\frac{1}{2}}}. \quad (54)$$

(The requirements $R\eta'' \ll S\eta, \eta'$ are equivalent to the less stringent condition $S \ll 1/R$.

Also, if in (53) we have $Kt_g \gg i$, i.e. perturbation growth which is slow relative to the elongation of the jet, the latter condition suffices.)

6. Results and discussion

The integro-differential equation for $\eta(\tau)$, (49), has been numerically integrated by a predictor–corrector routine, after reformulating it as a system of first-order ordinary differential equations.

In order to integrate (49) we need to specify the initial conditions for η and η', and the vorticity distribution at some initial time τ_0. It has been verified (Frankel 1984) that the initial vorticity distribution has only a minor effect on the evolution of perturbations. We therefore confine the following discussion to the case of zero initial vorticity and accordingly describe the solutions of the homogeneous equation associated with (49).

As in the case of an ideal jet (FW) it is found convenient to select the initial conditions

$$\tau = \tau_0: \quad \eta = \eta_0 = 1, \eta' = 0. \tag{55}$$

(No essential differences in the results occurred when other combinations were employed.)

The role of the parameter T which represents the relative effects of surface tension and the inertia of an inviscid liquid has already been extensively studied (FW). Thus, in all the following examples we select $T = 10$, which corresponds to both effects being of comparable magnitude, concentrating on viscosity effects (R). The influence of the parameter R is examined by presenting the results for $R = 0.1$, 1, and 10. These cover the range of values where the diffusion of vorticity and the elongation of the jet have comparable timescales.

6.1. *Evolution of perturbations*

To obtain some insight into the various mechanisms that affect the evolution of perturbations in the jet we compare the results of the numerical integration of the exact equation (49) (for the case of zero initial vorticity) with the following approximations:

(*a*) ideal liquid jet (32);

(*b*) viscous jet in the Stokes regime, (52) with S given by (51);

(*c*) irrotational viscous jet.

The latter is the solution for the equation

$$\frac{\tau^{\frac{1}{2}} I_0}{k_0 a_0 I_1}\eta''(\tau) + \left[-\frac{3}{2}\frac{1}{\tau^2} - \frac{2}{R} + \left(4\frac{\chi}{R} - \frac{1}{k_0 a_0 \tau^{\frac{1}{2}}}\right)\frac{I_0}{I_1} + \frac{3}{2}\frac{1}{\tau^2}\frac{I_0^2}{I_1^2}\right]\eta'(\tau)$$
$$-\frac{3}{4}\left[T\tau^{\frac{1}{2}}(1-\chi^2) - \frac{1}{\tau^3} + \frac{4\chi}{R\tau}\frac{I_0}{I_1}\right]\eta(\tau) = 0 \tag{56}$$

obtained by deleting the last term on the left-hand side of (49). Equation (56) is equivalent to an assumption of irrotational flow commonly used for an approximate evaluation of the effect of viscosity (e.g. the damping of the oscillations of liquid drops or of surface waves, cf. Lamb (1932, pp. 623–625 and 639–641, respectively) in the case of either small viscosity or the early development of a viscous flow which starts as an irrotational one.

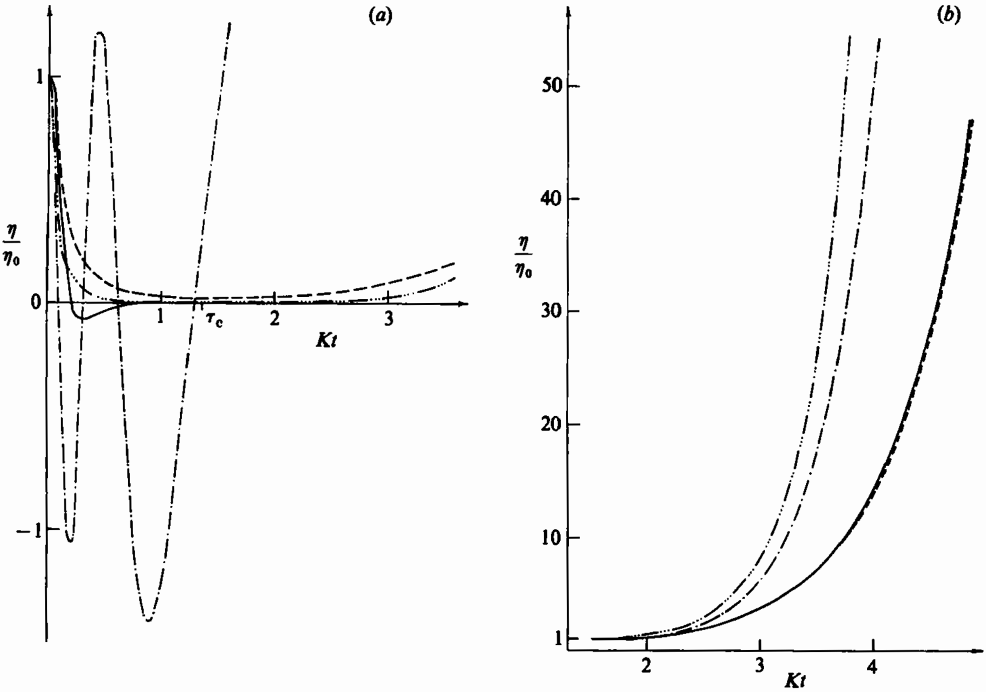

FIGURE 2. Comparison of the time variation of the amplitude according to the various solutions, for $T = 10$, $R = 1$, $k_0 a_0 = 4$, and (a) $\tau_0 = 1$, (b) 2.36: ——, solution of (49); ----, irrotational approximation: —·—·—, ideal jet; —···—···—, 'creeping flow' approximation.

Figure 2 shows the variation of the normalized amplitude, η/η_0, with the non-dimensional time $Kt(=\tau-1)$ according to the various models for $R = 1, T = 10$ and $k_0 a_0 = 4$. In (a) the evolution of perturbations that appear at $\tau_0 = 1$ $(t_0 = 0)$ is depicted.

η initially decreases in all the curves. This is because the destabilizing effect of surface tension is confined to non-dimensional wave-numbers $\chi < 1$. As a result of the disturbance wavelength growing in time, (19), all disturbances eventually enter the domain of destabilizing surface tension, yet perturbations with a short initial wavelength will grow monotonically only after a certain time has elapsed. (This phenomenon has been thoroughly discussed in FW for the case of an ideal liquid jet.)

The exact solution (full line) shows η to decrease rapidly at first, oscillate once and then decay. The calculation in this case was terminated when η became less than 10^{-7} for $\tau < \tau_c$. (τ_c is the smallest value of τ_0 for which the perturbations (55) grow monotonically.) When $\tau > \tau_c$ the solution turns unstable and thus even an infinitesimal residue of η will eventually grow, as with the other solutions shown in figure 2.

The 'irrotational' and 'creeping' approximations are more strongly damped. In both solutions the amplitude decreases at a slower rate than that of the exact solution, there are no oscillations, the amplitude is never completely damped, and eventually starts growing again for some $\tau > \tau_c$. We thus conclude that none of the approximations are reliable in the present case.

Figure 2(b) describes the various cases for the same values of R, T, and $k_0 a_0$, but for $\tau_0 = \tau_c = 2.36$. The irrotational approximation is almost indistinguishable from

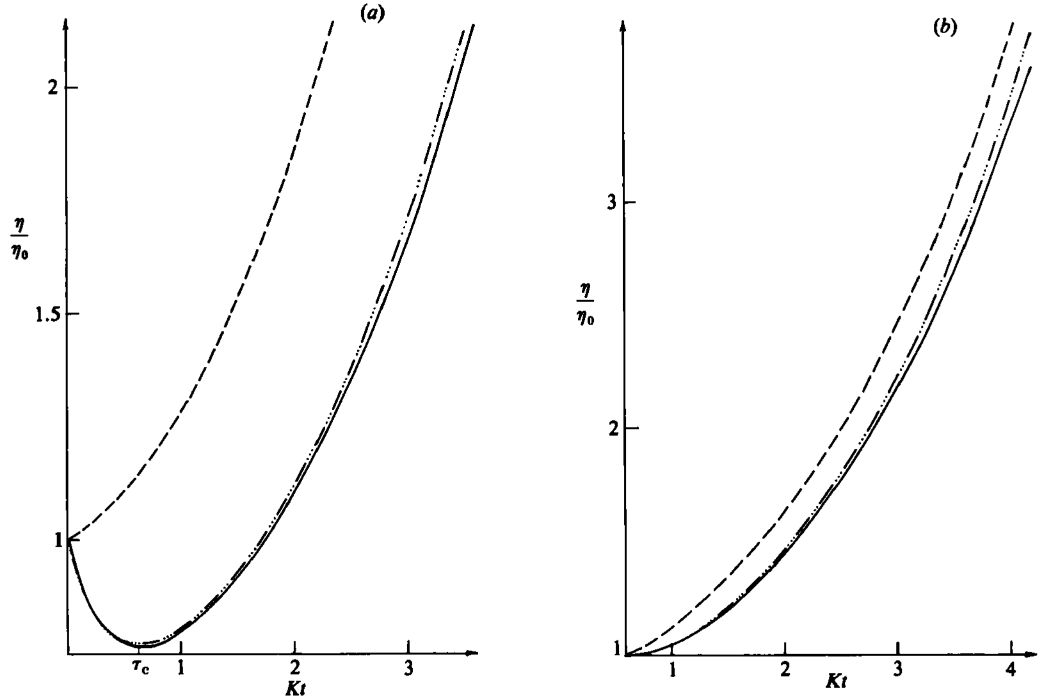

FIGURE 3. Same as figure 2, for $R = 0.1$, and (a) $\tau_0 = 1$, (b) 1.62.

the exact solution until $\tau \approx 5$. In this range of τ the dominant phenomenon seems to be the growth of perturbations under the destabilizing role of surface tension, whereas the role of vorticity distribution is of secondary importance.

Both the 'ideal' and 'creeping' solutions exhibit a significantly faster divergence since in each of these models one of the mechanisms that slow down the growth of perturbations (the viscous damping and the inertia of the liquid respectively) is missing.

For $\tau > 5$ $(Kt > 4)$ we see again that the irrotational model includes a stronger damping influence than the exact one: as mentioned above (the paragraph following (31)), the vorticity distribution contributes to the rate of dissipation within the jet. On the other hand this distribution tends to smooth the initial velocity gradients near the surface of the jet, thus diminishing the rate of dissipation there. The latter effect thus turns out to be the stronger one under the present circumstances.

Figure 3 describes the various solutions for $R = 0.1$, $T = 10$, $k_0 a_0 = 4$ and (a) $\tau_0 = 1$, or (b) $\tau_0 = \tau_c = 1.62$. The ideal solution, which has already been observed to constitute a poor approximation for $R = 1$ (cf. figure 2a), has been omitted here.

The 'creeping' model closely approximates the exact solution. Because $R \ll 1$, the irrotational solution is not even qualitatively correct in (a). (In (b) the difference is smaller since all the solutions show monotonical growth.)

Figure 4 displays the various solutions for $R = 10$, $T = 10$, $k_0 a_0 = 4$ and (a) $\tau_0 = 1$, or (b) $\tau_0 = \tau_c = 2.50$. In (a) the 'creeping' solution is critically damped and is essentially different from all the other solutions. The rest exhibit a somewhat similar behaviour: in the interval $\tau_0 \leqslant \tau \leqslant \tau_c$ they all oscillate with comparable frequencies, yet these oscillations are moderately amplified in the ideal case whereas in the other two they are gradually attenuated.

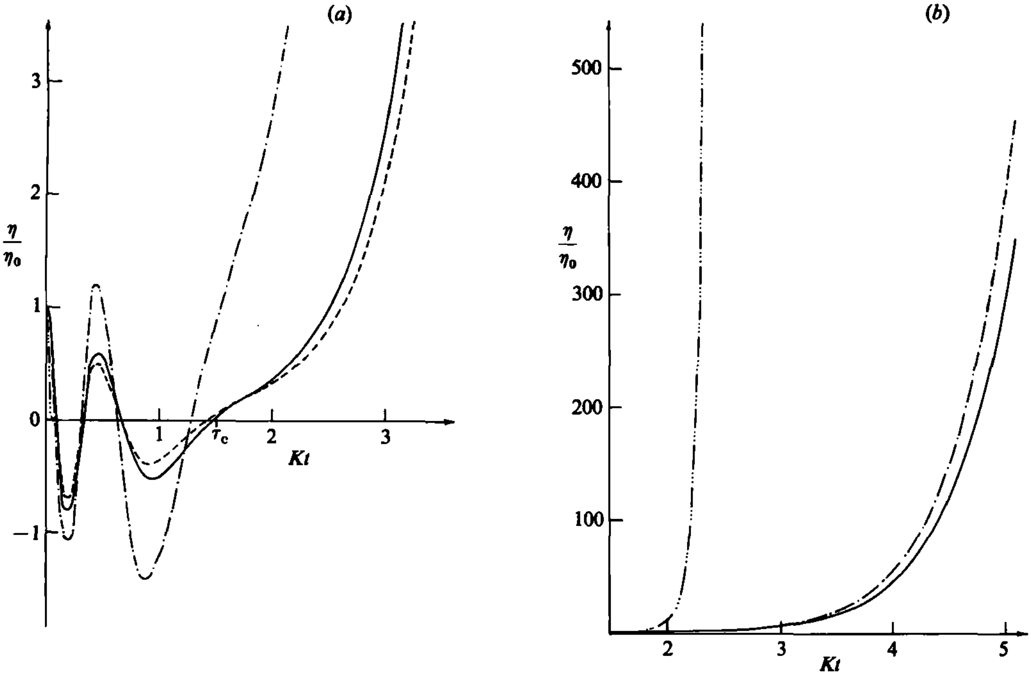

FIGURE 4. Same as figure 2, for $R = 10$, and (a) $\tau_0 = 1$, (b) 2.50.

For $\tau > \tau_c$ the ideal solution shows a much more rapid divergence. Again we note that the irrotational solution experiences a stronger damping than the exact one.

In (b) we see again that the 'creeping' solution deviates significantly from all the rest and exhibits a much sharper divergence. Its behaviour is described asymptotically (Frankel 1984) as

$$\frac{\eta}{\eta_0} \approx \tau \exp\left(\tfrac{1}{3} S \tau^{\frac{3}{2}}\right), \tag{57}$$

while in an ideal jet it is slower than simple exponential (FW).

The exact solution and the irrotational one are indistinguishable and are both relatively close to the ideal solution (as the viscous damping in the present example is much weaker than in the previous ones).

6.2. *Vorticity distribution*

The evolution of the vorticity distribution in the jet is governed by two time-dependent processes:

(a) the variations of the intensity of the vorticity source on the free surface associated with the variations in the amplitude of perturbations (cf. (30));

(b) the inward diffusion from the free surface.

Figure 5 describes the time dependence of the vorticity distribution for $T = 10$, $k_0 a_0 = 4$, $\tau_0 = 1$ and (a) $R = 1$, (b) $R = 0.1$, (c) $R = 10$. In the respective upper parts the perturbation amplitudes at the relevant instants of time are depicted.

In (a) the vorticity distribution is described at the times when $\Delta\tau = \tau - \tau_0 =$ (i) 0.005, (ii) 0.02, (iii) 0.06, (iv) 0.1, (v) 0.15, (vi) 0.3 and (vii) 0.4.

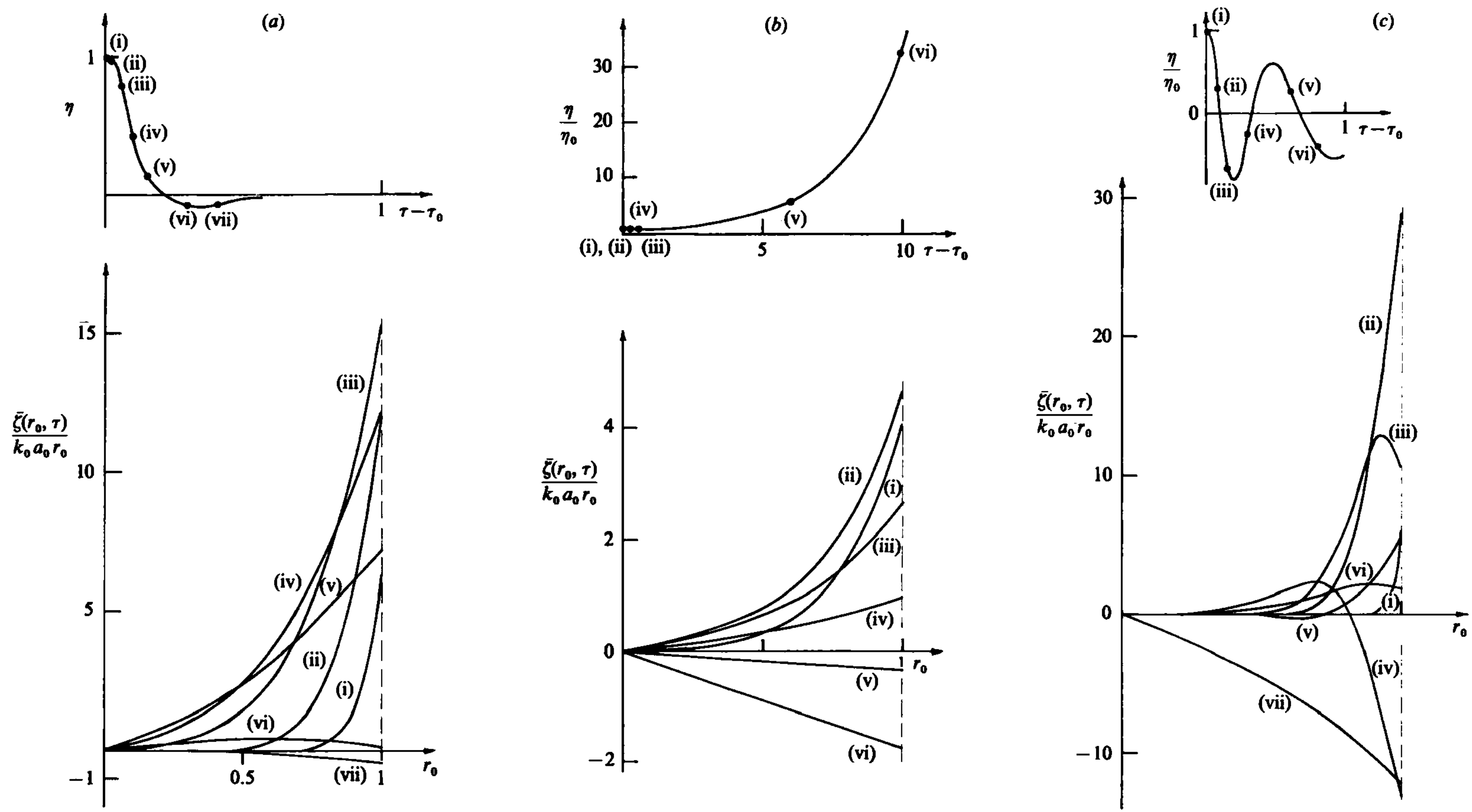

Figure 5. The time dependence of the vorticity distribution in the jet. The upper parts depict schematically the perturbation amplitude at the relevant instants of time. $T = 10$, $k_0 a_0 = 4$, $\tau_0 = 1$, $\Delta\tau = \tau - \tau_0$. (*a*) $R = 1$: (i) $\Delta\tau = 0.005$, (ii) 0.02, (iii) 0.06, (iv) 0.1, (v) 0.15, (vi) 0.3, (vii) 0.4. (*b*) $R = 0.1$: (i) $\Delta\tau = 0.005$, (ii) 0.02, (iii) 0.2, (iv) 0.6, (v) 6, (vi) 10. (*c*) $R = 10$: (i) $\Delta\tau = 0.005$, (ii) 0.08, (iii) 0.15, (iv) 0.3, (v) 0.6, (vi) 0.8, (vii) 4.

During the transition (i)–(ii)–(iii) we see that the source strength increases (η slightly decreases while η', which was $\eta' = 0$ at $\tau = \tau_0$, becomes $\eta' < 0$) while the vorticity diffuses into an increasing portion of the jet.

In the times (iv)–(v)–(vi) the source intensity diminishes (η decreases while η' gradually increases). Owing to the time lag in the diffusion process, we see that the vorticity in the inner portion of the jet is larger at time (v) than (iv) (although the source strength has meanwhile been significantly reduced).

At time (vii) the source strength turns negative ($\eta < 0, \eta' > 0$). Later on the surface perturbations vanish and the vorticity is damped.

Figure 5(*b*) displays the vorticity distribution when: $\Delta\tau = \tau - \tau_0 =$ (i) 0.005, (ii) 0.02, (iii) 0.2, (iv) 0.6, (v) 6, (vi) 10.

Between points (i) and (ii) there is some increase in the source intensity ($\eta' < 0$). At the relatively short time ($\Delta\tau = 0.02$) which corresponds to (ii) there is already a significant vorticity even in the inner portion of the jet.

Later on ((ii)–(iii)–(iv)) the source intensity decreases at a moderate rate, changes its sign (v) and then monotonically increases in its absolute value (along with the divergence of the surface perturbations).

Unlike (*a*), the vorticity does not die down: owing to the higher damping, the surface perturbations do not vanish until the range of divergence is reached. In addition, no time-lag phenomena (associated with the diffusion of vorticity, e.g. curve (v) in *a*) are seen here.

In (*c*) the vorticity distribution is depicted at the instants $\Delta\tau = \tau - \tau_0 =$ (i) 0.005, (ii) 0.08, (iii) 0.15, (iv) 0.3, (v) 0.6, (vi) 0.8, (vii) 4. This case ($R = 10$) is characterized relative to the previous ones ($R = 0.1, 1$) by both the oscillations in the source intensity (associated with oscillations of the surface perturbations prior to the appearance of the (monotonical) divergence, cf. figure 4*a*), and the significant time lag in the diffusion process.

From (i) to (ii) the source intensity increases substantially ($\eta' < 0$) and vorticity starts penetrating the jet. At (iii) the source strength has been greatly reduced, yet owing to the time lag in the diffusion process there appears a distinct maximum in the distribution, at $r_0 = 0.93$.

At (iv) there is a further decrease of the source intensity which becomes negative ($\eta' > 0$). Owing to the damping its absolute value is smaller than at (ii). In a major portion of the jet we see vorticity of the opposite sense (positive) relative to the instantaneous surface source strength.

As a result of the oscillations of the surface perturbations, the source intensity turns positive again (v) (with a region of negative vorticity), its strength diminishes (vi) (with a maximum at $r_0 = 0.9$) and later turns negative (vii). After this point the oscillations cease, the surface perturbations become monotonically divergent (cf. figure 4*a*) and there is a corresponding monotonical increase in the absolute value of vorticity.

It is remarkable that during the time up to $\Delta\tau = 0.8$ (curve vi) a significant part of the jet ($0 \leqslant r_0 \leqslant 0.3$) remains irrotational. This is a joint effect of the oscillations and the relatively slow vorticity diffusion. A characteristic length for the spread of vorticity (e.g. Lamb 1932, p. 620) is $\delta \approx (\nu/\omega)^{\frac{1}{2}}$, where ω is the frequency of oscillation. In the case of oscillation induced by surface tension, $\omega \approx (\sigma/\rho a_0)^{\frac{1}{2}}$, and thus we obtain $\delta/a_0 \approx (\frac{3}{4}R^2T)^{-\frac{1}{4}} \approx 0.19$, when substituting the definitions of R and T and the relevant data.

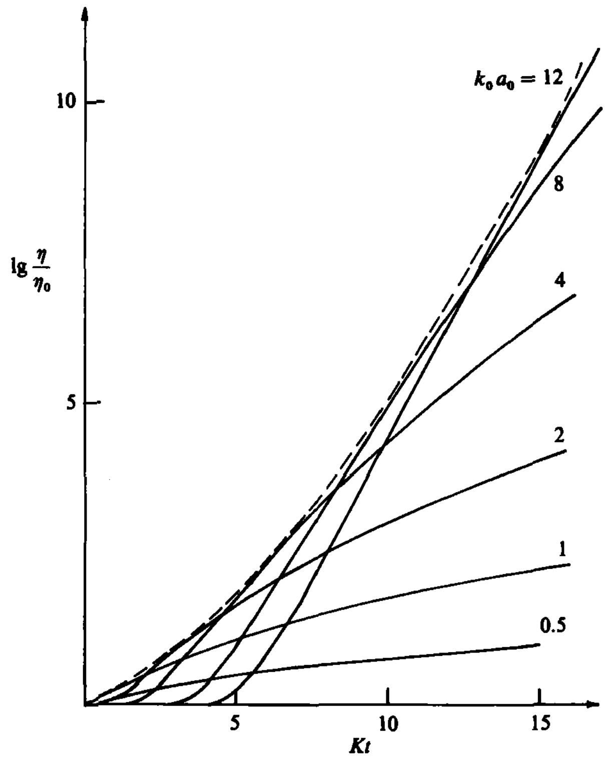

FIGURE 6. The effect of $k_0 a_0$ on the time dependence of amplification for $T = 10$, $R = 1$. The broken line shows the 'amplification envelope'.

6.3. *Dependence of amplification on wavelength*

Since perturbations can appear in the jet at all times $\tau_0 \geqslant 1$, the parameter $k_0 a_0$ does not correspond to a single perturbation, but rather to the whole spectrum of perturbations each of which attains an instantaneous wavenumber of $\chi = k_0 a_0/\tau^{\frac{3}{2}}$. The total growth of perturbations which belong to the same $k_0 a_0$ but are introduced in the flow at different values of τ_0 can differ markedly (cf. figures 2–4). Thus in order to study the effect of the wavelength, it is desirable to select a single perturbation from the spectrum which corresponds to a specific value of $k_0 a_0$.

It is most interesting and convenient to examine the earliest perturbations that grow monotonically (with the corresponding τ_0 denoted by τ_c). For each $k_0 a_0$ these are also the perturbations of maximal amplification.

Figure 6 describes the dependence of the amplification of the selected perturbations on the non-dimensional time $Kt = \tau - 1$, for $T = 10$, $R = 1$, and several values of $k_0 a_0$. We see that the greater the value of $k_0 a_0$, the larger the corresponding amplification, and the later this amplification appears. Consequently there is no single dominant perturbation throughout the process, i.e. there is a different dominant perturbation at each time.

Figure 7 shows the time variation of the maximal amplification $M = \lg_{10}(\eta/\eta_0)_{\max}$ for $T = 10$ and $R = 0.1$, 0.3, 1, 10 as well as the limiting cases $R \rightarrow 0, \infty$. The curve $R = 1$ is identical with the 'amplification envelope' marked by the broken line in figure 6. The curves $R = 0.1$, 0.3, 10 are obtained in a similar manner. The curve for $R \rightarrow \infty$ corresponds to the solution for an ideal liquid jet, (32), whereas the curve for $R = 0$ is obtained from the 'creeping flow' approximation, (52), with $S = 0$.

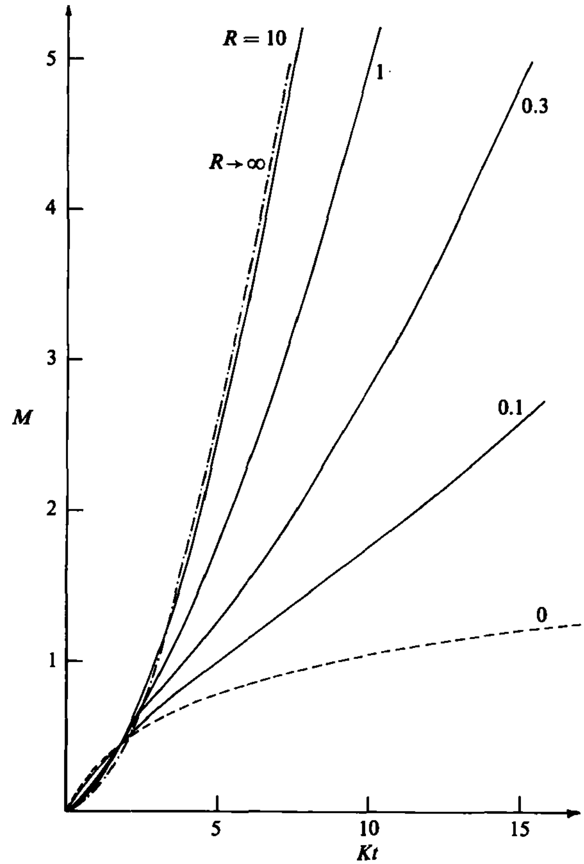

FIGURE 7. The effect of R on the time dependence of M, the maximum amplification for $T = 10$: ——, $R = 0.1, 0.3, 1, 10$; —·—·—, $R \to \infty$; ----, $R = 0$.

The curves for $R = 10$ and $R \to \infty$ are fairly close, i.e. for $R = 10$ the evolution of perturbations which appear at $\tau_0 \geqslant \tau_c$ in the viscous jet is very much the same as in an ideal jet. This observation is confirmed by figure 4(*b*) (while part 4*a* shows marked differences when $\tau_0 < \tau_c$).

An interesting feature of the flow revealed by the figure is the dual role played by the viscosity in the elongating jet: in addition to the usual damping effect it has also a destabilizing influence. We see that at long times ($Kt > 2$) M is increasing with the value of R, yet this trend is reversed at short times ($Kt < 2$). The amplification becomes largest for $R = 0$. Thus, at early times viscosity has a destabilizing effect which accelerates the initial growth of perturbations. Later on, when the perturbations are rapidly diverging, the damping mechanism sets in and tends to slow down the growth. The relative importance of both effects increases with decreasing values of R.

In order to pinpoint the physical mechanism for the destabilizing effect of viscosity, we consider the elongational flow in the case where both inertia and surface tension vanish ($\rho = 0$ and $\sigma = 0$, respectively). In the unperturbed flow the viscous stresses are $\tau_{zz} = 3\mu K/Kt+1$. The corresponding resultant axial force, $F_z = \pi a^2 \tau_{zz} = 3\pi a^2 \mu K/Kt+1$, is uniform along the jet.

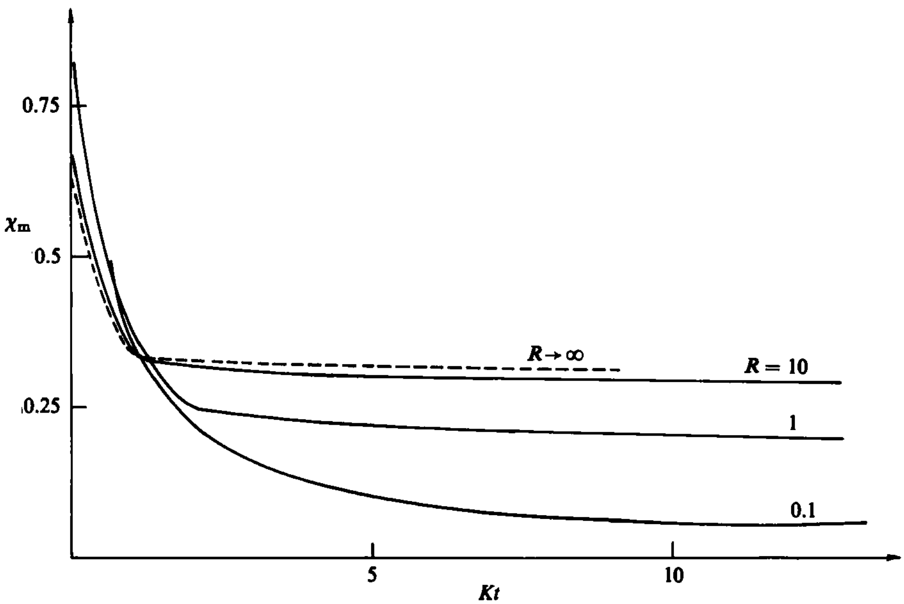

FIGURE 8. The influence of R on the time dependence of χ_m, the instantaneous wavenumber of the dominant perturbations for $T = 10$.

The combined effect of the basic velocity field and perturbed jet surface (with $a(t)$ being replaced by $b(z,t)$, (23)) results in an increment to F_z in the form of

$$\Delta F_z \approx 6\frac{\pi a^2 \mu K}{Kt+1}\eta \cos kz. \tag{58}$$

To see that this longitudinal distribution of the axial force is destabilizing, consider a thin 'slice' of the perturbed jet (normal to its axis). Owing to the above distribution, the resultant axial force on the slice tends to move it away from the nearest 'neck', and thus tends to further increase the perturbation amplitude η.

The conclusion that perturbations can grow due to the effect of viscosity, even in the absence of surface tension, can also be reached from the asymptotic result (57). When we substitute $S = 0$ we obtain $\eta/\eta_0 \approx \tau$, i.e. an 'algebraic' growth. This is also supported by the behaviour of the curve $R = 0$ in the figure.†

Figure 8 describes the time dependence of χ_m, which corresponds to the instantaneous perturbation of maximal growth, for $T = 10$ and $R = 0.1$, 1, 10 and ∞ (ideal jet).

All the curves show χ_m to decrease rapidly at small times and then tend to constant asymptotic values. These features have already been observed for the inviscid case (FW). Here we focus our attention on the R-dependence of χ_m. The qualitative difference between the respective effects of R at short and long times is again related to the dual role of viscosity.

The destabilizing mechanism appears at early times. The magnitude of the destabilizing axial force which results from the distribution (58) is independent of the perturbation wavelength. Yet, the shorter this wavelength, the smaller is the liquid

† For a given T, $R \to 0$ corresponds to $S = 0$, i.e. the effect of surface tension becomes negligible relative to that of the viscosity.

mass that has to be accelerated by the viscous force in order to amplify the perturbation. Consequently χ_m increases with decreasing values of R.†

At later times the effect of viscosity is essentially a damping one which is stronger the shorter the perturbation wavelength. Thus χ_m increases with increasing values of R.

Again we observe only slight differences between the curves $R = 10$ and $R \rightarrow \infty$, which confirms our earlier conclusion that even for $R = 10$ the jet behaviour closely resembles that of an ideal jet.

7. Concluding remarks

The present solution includes both the effect of the inertia of the liquid and that of its viscosity, in the case of an elongating capillary jet, thereby constituting a generalization of previous solutions which have neglected either the inertia of the jet or its viscosity.

Owing to the basic elongational flow the time dependence of the perturbations is not simply exponential. Consequently we need to solve the initial-value problem for the time evolution of perturbations (instead of an eigenvalue problem as in the case of a non-stretching jet). The evolution equation turns out to be an integro-differential one owing to the time lag in the diffusion of vorticity.

The solutions of the evolution equation show that perturbations can change their mode of behaviour: perturbations with a short initial wavelength can start as oscillating ones and become monotonically divergent later on. Another result which is also related to the 'stretching' of the wavelengths of perturbations is that there is a different dominant perturbation at each instant of time.

The effect of viscosity relative to that of the inertia of the liquid is represented by the parameter R^{-1}. It is found to play a dual role: a destabilizing one and a damping one. The destabilizing influence manifests itself as a tendency to amplify perturbations in the early stages of their development which results in extending the wavelength range where perturbations can diverge monotonically. The damping role appears at a later stage when the perturbations are rapidly diverging. Both effects are more pronounced the smaller the value of R and the shorter the wavelength.

Such improved understanding of the stability of stretching jets can be applied to practical cases where jet breakup is to be accelerated (as in protection from shaped charges – Mayseless *et al.* 1984).

REFERENCES

ABRAMOWITZ, M. & STEGUN, I. A. 1965 *Handbook of Mathematical Functions*. Dover.

BATCHELOR, G. K. 1967 *An Introduction to Fluid Dynamics*. Cambridge University Press.

BIRKHOFF, G., MACDOUGALL, D. P., PUGH, E. M. & TAYLOR, G. I. 1948 Explosives with lined cavities. *J. Appl. Phys.* **19**, 563–582.

FRANKEL, I. & WEIHS, D. 1985 Stability of a capillary jet with linearly increasing axial velocity (with application to shaped charges). *J. Fluid Mech.* **155**, 289–307.

FRANKEL, I. 1984 Flow and stability in liquid jets with longitudinal distribution of axial velocity. PhD thesis, Technion, Haifa.

† The range of 'unstable wavelengths' is limited to $\chi < \chi_c$. Owing to the effect of viscosity this range is extended to $\chi_c > 1$ (depending on the value of R) while for a non-stretching jet $\chi_c = 1$, and in the case of an ideal elongating jet (FW) it is further limited to $\chi_c < 1$ (depending on the value of T).

GOLDSTEIN, S. 1932 Some two dimensional diffusion problems with circular symmetry. *Proc. Lond. Math. Soc.* **34**, 51–88.

GRAY, A., MATHEWS, G. B. & MACROBERT, T. M. 1922 *A Treatise on Bessel Functions and Their Applications to Physics*, 2nd edn. Macmillan.

LAMB, H. 1932 *Hydrodynamics*, 6th edn. Cambridge University Press. (Reprinted by Dover 1945.)

MAYSELESS, M., ERLICH, Y., FALCOVITZ, Y., ROSENBERG, G. & WEIHS, D. 1984 Interaction of shaped charge jets with reactive armor. In *Proc. 6th Intl Symp. on Ballistics, Orlando, Fl.*, pp. 7-15 to 7-20. American Defense Preparedness Association.

MIKAMI, T., COX, R. G. & MASON, S. G. 1975 Breakup of extending liquid threads. *Intl J. Multiphase Flow* **2**, 113–138.

PROSPERETTI, A. 1976 Viscous effects on small amplitude surface waves. *Phys. Fluids* **19**, 195–203.

PROSPERETTI, A. 1980 Free oscillations of drops and bubbles, the initial value problem. *J. Fluid Mech.* **100**, 333–347.

ROSENHEAD, L. 1963 *Laminar Boundary Layers*. Oxford University Press.

TOMOTIKA, S. 1936 Breaking up of a drop of viscous liquid immersed in another viscous fluid which is extending at a uniform rate. *Proc. R. Soc. Lond.* A **153**, 302–318.